ACS OMEGA

Article

http://pubs.acs.org/journal/acsodf

Enhanced Carbon Nanotubes Growth Using Nickel/Ferrocene-Hybridized Catalyst

Yu Dian Lim,[†] Alexander Vasiliyvich Avramchuck,[‡] Dmitry Grapov,[‡] Chong Wei Tan,[†] Beng Kang Tay,*[,†] Sheel Aditya,[†] and Vladimir Labunov[‡]

[†]School of Electrical and Electronics Engineering, Nanyang Technological University, 50 Nanyang Avenue, 639798 Singapore

[‡]Micro- and Nanoelectronics Department, Belarusian State University of Informatics and Radioelectronics, vulica Pietrusia Broŭki 6, 220013 Minsk, Belarus

ABSTRACT: Tall, crystalline carbon nanotubes (CNTs) are desired to successfully integrate them in various applications. As the crystallinity of CNTs improves with increasing growth temperatures, higher growth temperatures are required to obtain crystalline CNTs. However, in a typical chemical vapor deposition (CVD) process, CNT growth rate reduces when the growth temperature exceeds a specific level due to the degradation of the catalyst particles. In this study, we have demonstrated the improved catalytic activity of nickel/ferrocene-hybridized catalyst as compared to sole ferrocene catalyst. To demonstrate this, CNTs are grown on bare silicon (Si) as well as nickel (Ni) catalyst-deposited substrates using volatile catalyst source (ferrocene/xylene) CVD at the growth temperatures ranging from 790 to 880 °C. It was found that CNTs grown on bare Si substrate experience a reduction in height at growth temperature above 860 °C, whereas the CNTs grown on 10 nm Ni catalyst-deposited substrates experience continuous increase in height as the temperature increases from 790 to 880 °C. The enhancement in the height of CNTs by the addition of Ni catalyst is also demonstrated on 5, 20, and 30 nm Ni layers. The examination of CNTs using electron microscopy and Raman spectra shows that the additional Ni catalyst source improves the CNT growth rates and crystallinity, yielding taller CNTs with a high degree of structural crystallinity.

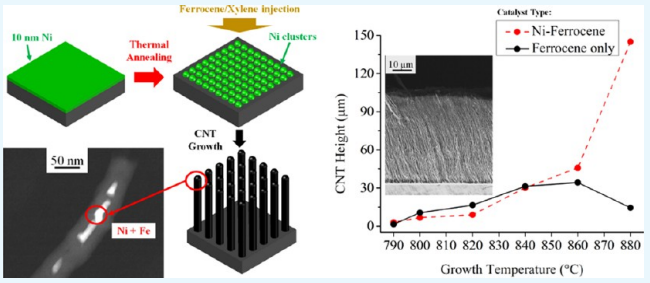

INTRODUCTION

Since the discovery of carbon nanotubes (CNTs) by Iijima,[1] there has been an ongoing interest in the properties and the synthesis techniques for CNTs. Comprehensive understanding of CNTs is required for their successful integration into the applications that utilize their unique properties, including high mechanical strength,[2] high aspect ratio,[3] and outstanding electrical properties.[4] These applications include field emission devices,[5] separation science,[6] miniaturized interconnects and passives,[7] energy storage,[8] biomedical membrane,[9] and so on, which have been proposed extensively in the past decade. Among the reported potential applications, there has been increasing interest in the application of CNTs in electronic interconnects due to their outstanding electrical conductivity.[10,11] At the same time, CNTs also show promise in field emission applications due to their exceptionally high aspect ratio and unique electrical properties.[12] To integrate CNTs in these applications, tall CNT pillars with specified degree of crystallinity are needed.[13,14] For instance, crystalline CNTs with substantial height are needed for realizing an efficient bottom-up filling of the via holes in miniatured interconnects;[15] moreover, tall, high-aspect-ratio CNTs are required in field emission applications to achieve high emission current density.[16]

In a typical chemical vapor deposition (CVD) process for growing CNTs, the widely accepted growth model assumes that the hydrocarbon vapor is absorbed by the catalyst nanoparticles formed from thermal annealing and catalytically decomposed carbon species are diffused through the catalyst nanoparticles. Upon reaching supersaturation, carbon structure will be precipitated out in the form of seamless carbon cylinder.[17] To achieve highly crystalline CNTs, it has been reported that the growth temperature of CNTs plays a significant role in their crystallinity.[18,19] However, a common issue in obtaining tall, crystalline CNTs is the reduction of CNT growth rate at high temperatures due to the reduction in the catalytic activity.[20,21] This reduction in the CNT growth rate will lead to the formation of shorter CNTs, which limits their performance in applications where tall, crystalline CNTs are required.

It has been commonly reported that the reduction of CNT growth rate at high growth temperatures can be attributed to the catalyst-poisoning phenomenon wherein catalyst particles are deactivated due to the encapsulation of catalyst particles by amorphous carbon.[21,22] This encapsulation will result in limiting the diffusion of hydrocarbon source into the catalytic

Received: June 24, 2017
Accepted: September 7, 2017
Published: September 21, 2017

DOI: 10.1021/acsomega.7b00858
ACS Omega 2017, 2, 6063−6071

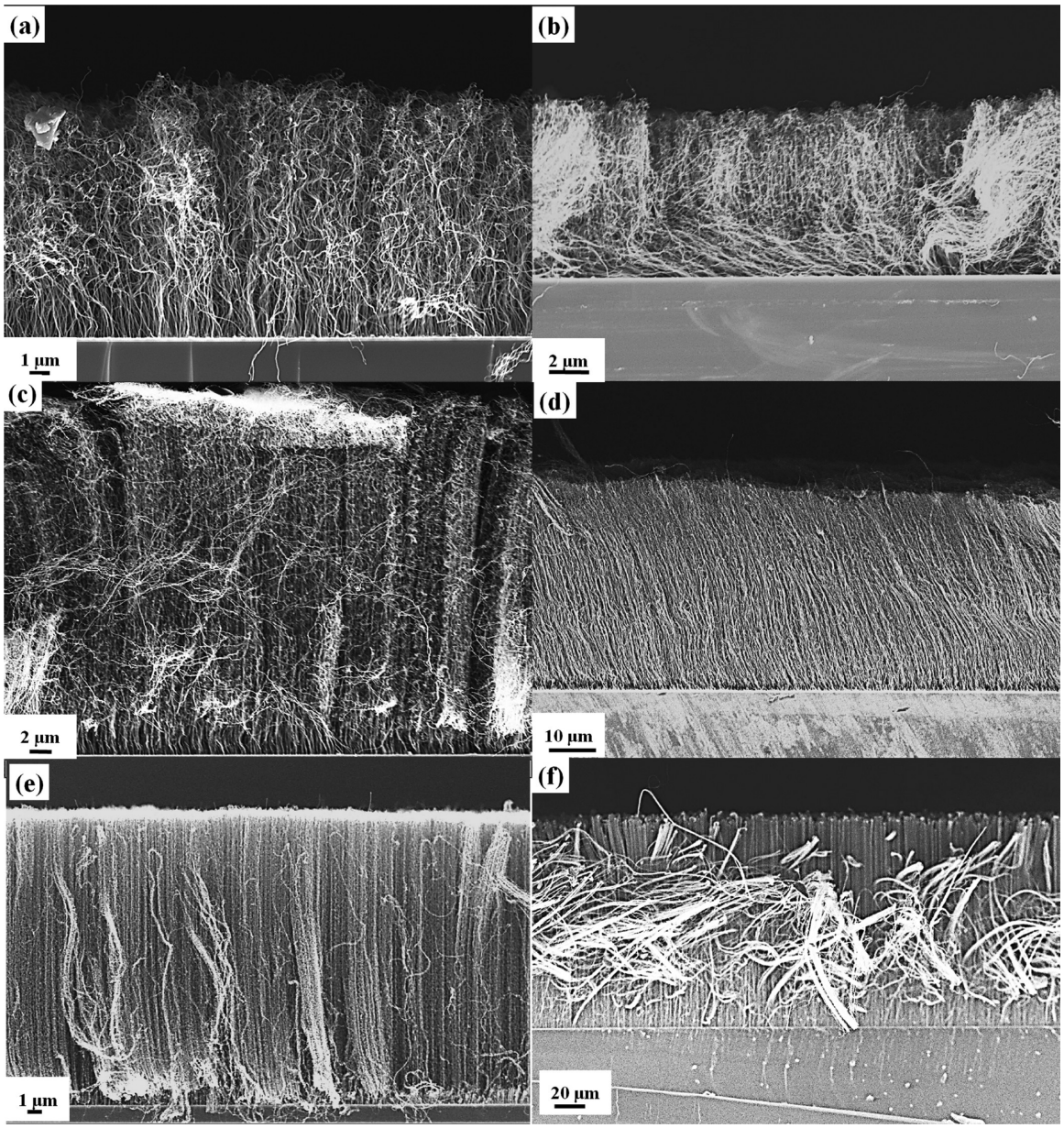

Figure 1. SEM images of CNT grown on (a) bare Si and (b) 10 nm Ni substrates at 800 °C, (c) bare Si and (d) 10 nm Ni substrates at 860 °C, and (e) bare Si and (f) 10 nm Ni substrates at 880 °C.

particles, hindering the nucleation of carbon particles to form CNTs.[23] However, it has been reported by Xiang et al. that the decreasing growth of CNTs cannot be solely attributed to the diffusion limit of hydrocarbon into the catalyst nanoparticles, as suggested by the simulated and the experimental outcomes.[24] At the same time, Schünemann et al. have suggested that the catalyst-poisoning phenomenon does not give a comprehensive explanation of the reduction of CNT growth rate at higher growth temperatures and needs to be re-examined. Nevertheless, the reduction in the CNT growth rate can be attributed to various factors such as the nucleation rate of catalytic particles, diffusion of the hydrocarbon source during CVD growth, hydrogenation activity on the precipitated carbon encapsulation, and so on.[25]

From the reported literatures, catalyst enhancement in the CNT growth can be carried out using two different approaches, reducing the carbon encapsulation on the catalyst particles and enhancing the CNT yield using mixed catalyst sources. To reduce carbon encapsulation, introduction of etching agent (H_2) has been reported to prevent the encapsulation of catalyst particles by carbon precipitation.[23,26] Besides using H_2 etching agent, Patole et al. also reported supergrowth of CNTs using water-assisted CVD. In the reported study, water was used as a weak oxidizing agent to remove the amorphous carbon coating around the catalyst particles, lengthening the lifetime of the catalyst.[27] Apart from etching and oxidation to remove carbon encapsulation, Liu et al. have reported the use of novel nanoarchitectured Co/Pt/Au catalyst. The use of nanostructured Co/Pt/Au catalyst has been reported to reduce the formation of carbon encapsulation around the catalytic particles.[28]

In the use of mixed catalyst sources, it has been reported that depositing nickel catalyst layer on the predeposited iron catalyst layer promotes a higher CNT yield[29] due to a high

DOI: 10.1021/acsomega.7b00858
ACS Omega 2017, 2, 6063−6071

hydrocarbon decomposition rate.[30] Besides using bilayer nickel/iron catalyst, Atthipalli et al. have reported use of hybridized catalyst combining the predeposited nickel layer and continuously injecting volatile ferrocene catalyst sources for dense, vertically aligned CNT growth.[31,32] As ferrocene is an iron-containing organometallic compound, using ferrocene/nickel-mixed catalyst source resembles the use of iron/nickel-mixed catalyst, as discussed earlier. It can be predicted that the additional catalytic activity of nickel to the ferrocene catalyst source contributes significantly to the achievable CNT height and the crystallinity in a CVD process. However, the comparative growth between the sole ferrocene catalyst source and the nickel/ferrocene-hybridized catalyst source is not addressed in the reported studies by Atthipalli et al. At the same time, there still exist limited comparative studies between the hybridized catalyst sources and other catalyst sources.

In this study, the goal is to investigate the effect of adding nickel catalyst to the volatile ferrocene catalyst source in the CNT growth. We have performed a temperature-dependent comparative study between use of the sole ferrocene catalyst source and the nickel/ferrocene-hybridized catalyst sources in the CNT growth. We have demonstrated that CNTs grown using sole ferrocene catalyst source experience reduction in height above a specific growth temperature. On the other hand, the CNTs grown using nickel/ferrocene-hybridized catalyst source experience a continuous increase in height with increase in temperature. This suggests that the additional nickel catalyst enhances the catalytic activity of the ferrocene catalyst source. The use of nickel/ferrocene-hybridized catalyst sources promotes tall, vertically aligned crystalline CNTs that are desired for applications where these conditions are required.

RESULTS AND DISCUSSION

For all of the experiments, the chemical vapor deposition (CVD) growth temperature is varied between 790 and 880 °C on the nickel-deposited (10 nm Ni) and bare silicon (Si) substrates, keeping all of the other parameters constant. The CNTs show poor alignment for 800 °C growth temperature on both 10 nm Ni and bare Si substrates, as shown in Figure 1a,b. As the growth temperature increases to 860 °C, the CNT alignment improves, as shown in Figure 1c,d. As the growth temperature further increases to 880 °C, homogeneous, vertically aligned CNT films are obtained on both 10 nm Ni and bare Si substrates, as seen in Figure 3e,f. Despite the appearance of detached CNTs, it can be seen that tall (145 μm), vertically aligned CNTs are grown on 10 nm Ni substrate at 880 °C growth temperature (Figure 1f). The CNT alignment is highly dependent on the "crowding effect" between CNTs, where the densely packed CNTs show a high degree of vertical alignment due to the mechanical support between CNTs.[33] At higher growth temperatures, the catalyst nanoparticles size distribution is small and homogeneous;[34] the small diameter, high-density CNTs grown from the small catalyst nanoparticles are afflicted with high Van der Waals interactions, which results in the vertical alignment of CNTs.[35]

The Raman characteristics of CNTs grown at different temperatures on 10 nm Ni and bare Si substrates are shown in Figure 2. The appearance of the D band (1339−1444 cm^{-1}) and G band (1575−1577 cm^{-1}) in the Raman spectrum for all of the investigated CNT samples indicate the presence of a disorder in the graphitic structure and the in-plane vibration of the C−C bond.[36] Generally, CNTs show an increasing degree of crystallinity (decreasing I_d/I_g ratio) as the growth temperature increases. This agrees well with Lee et al., who showed that the degree of crystalline perfection in the CNTs increases progressively as the growth temperature increases.[19] Overall, the CNTs grown on 10 nm Ni substrate show a higher degree of crystallinity (lower I_d/I_g ratio) at higher growth temperatures. This improvement in the degree of crystallinity can be attributed to the catalytic effect by Ni, as suggested by Hoyos-Palacio et al.[37]

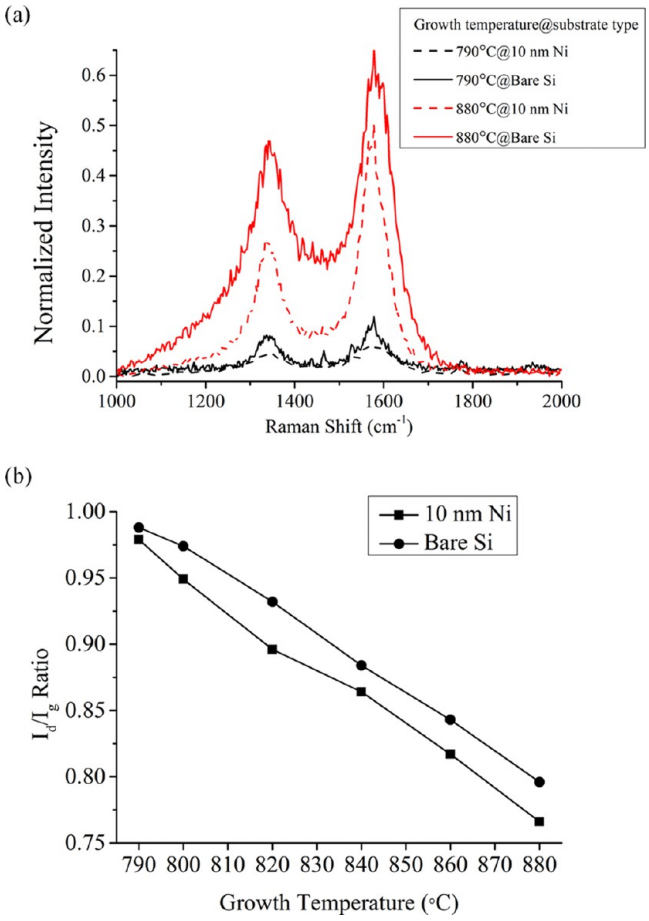

Figure 2. (a) Raman spectrum of the CNTs grown on bare Si and 10 nm Ni substrates at 790 and 880 °C; (b) I_d/I_g ratio of CNTs grown on bare Si and 10 nm Ni substrates at the growth temperatures between 790 and 880 °C.

To investigate the effect of growth temperature on the CNT height, we have compiled the CNT height−growth temperature profiles for the CNT grown on 10 nm Ni and bare Si substrates, as shown in Figure 3. On the bare Si substrate, it is shown that the obtained CNT height−growth temperature profiles possess a similar trend as that reported by Bai et al., wherein the CNTs reach a maximum height at a specific temperature and the height reduces as the growth temperature increases further.[21] As shown in Figure 3, the CNT height increases from 1.45 to 31.32 μm on the bare Si substrate as the growth temperature rises from 790 to 840 °C. This increment of the CNT height can be attributed to the higher decomposition rate of ferrocene at a higher temperature, which increases the catalytic effect of ferrocene.[16] The CNT height reaches a saturation point of 34.28 μm at 860 °C. As the temperature increases further to 880 °C, the CNT height reduces to 17.4 μm due to the encapsulation of catalyst nanoparticles by hydrocarbon precipitates,[38] as predicted by Bai

DOI: 10.1021/acsomega.7b00858
ACS Omega 2017, 2, 6063−6071

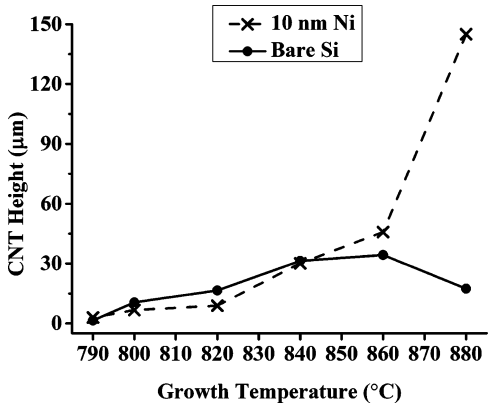

Figure 3. CNT heights on bare Si and 10 nm Ni substrates at different growth temperatures.

et al.[21] In contrast, the CNT height on 10 nm Ni substrate increases continuously with increase in the CVD growth temperature from 790 to 880 °C. At 880 °C, much taller CNTs are formed on 10 nm Ni substrate (145 μm) as compared with CNTs formed on bare Si substrate (17.4 μm).

To further justify the improvement in CNT heights by additional Ni catalyst, we have repeated the CNT growth process on Ni catalyst of different thickness, using the obtained optimal growth temperature of 880 °C. Figure 4 presents the SEM images of the CNTs grown on 5, 20, and 30 nm Ni catalyst and the variation of obtained CNT heights on different Ni thicknesses. From the SEM images, it can be observed that the CNTs grown on 5, 20, and 30 nm Ni catalyst show a vertical alignment, similar to the CNTs obtained on the 10 nm Ni catalyst as exhibited in Figure 1. Among the investigated Ni thickness, the tallest CNTs are grown from 5 nm Ni catalyst. As the thickness of Ni catalyst increases, the shorter CNTs are obtained. This obtained outcome is similar to several reported studies,[39−41] wherein the CNT growth rate reduces with increase in the catalyst thickness. To explain this outcome, Jang et al. suggested that variation in the CNT heights with catalyst thickness can be attributed to the carbon diffusion length in catalyst particles. For a thicker catalyst, the diffusion length of carbon increases with decrease in the growth rate, resulting in shorter CNTs.[42] Nevertheless, in this study, the CNTs grown from 5 to 30 nm Ni catalyst layer are generally taller than the CNTs grown from pure ferrocene catalyst. From the obtained CNT heights, it can be postulated that the formation of taller CNTs on the Ni substrates is due to the additional assistance of the Ni catalyst to the Fe catalyst from ferrocene.

For further verification of the above-mentioned postulation, we have performed the transmission electron microscopy (TEM) and energy-dispersive X-ray spectroscopy (EDS) characterizations on the CNT samples grown on bare Si and 10 nm Ni substrates. Multiple metal clusters are found on the CNTs grown on both bare Si and 10 nm Ni substrates (Figure 5a,d). The tubular and multiwalled structure of the CNTs on bare Si and 10 nm Ni substrates can be seen in Figure 5b,e. The obtained structure of CNTs possesses similar morphological properties as reported by Kar et al.[43] CNTs grown on 10 nm Ni substrate show a larger diameter (50.7 nm outer diameter; 16.3 nm inner diameter) as compared to the CNTs grown on bare Si substrate (20.8 nm outer diameter; 10.2 nm inner diameter). As shown in Figure 5c,f, the metal clusters are found on the tips of CNTs on bare Si and 10 nm Ni substrates. On both 10 nm

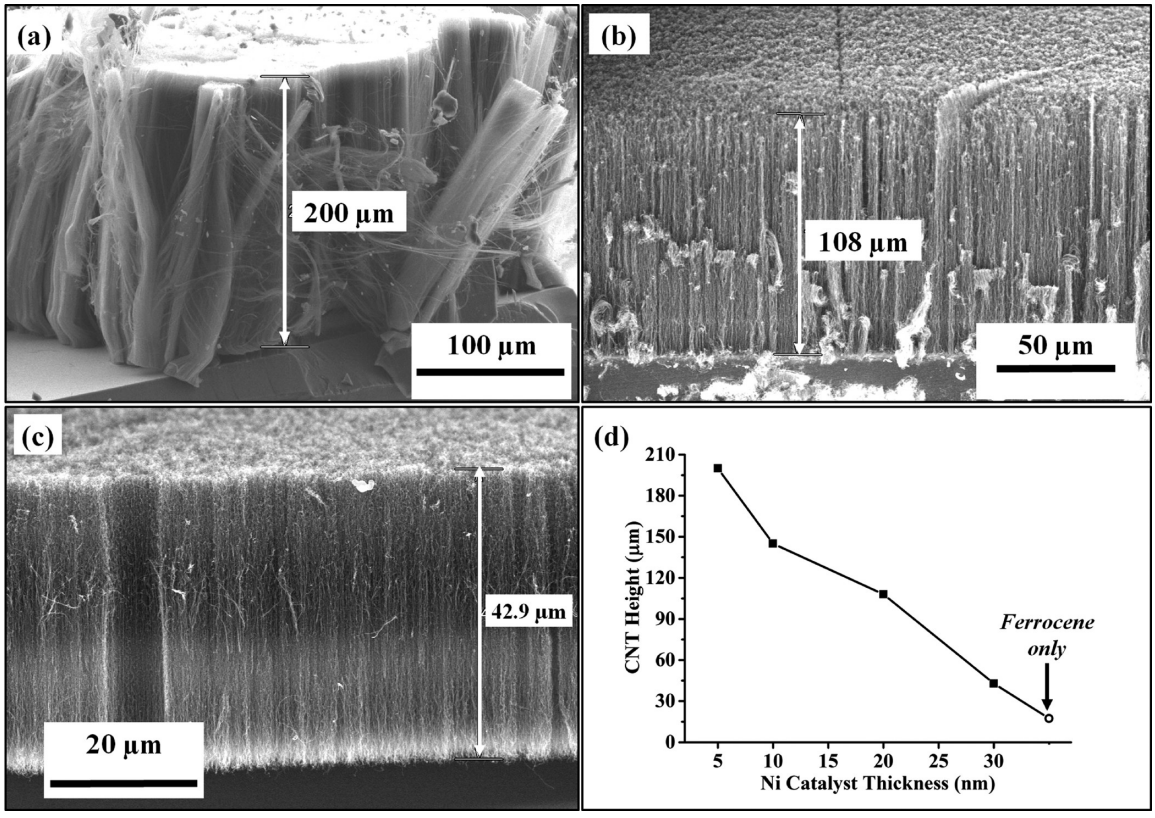

Figure 4. SEM images of CNTs grown using (a) 5 nm, (b) 20 nm, and (c) 30 nm thick Ni catalyst at 880 °C growth temperature. (d) Variation in the CNT heights with Ni catalyst thickness.

DOI: 10.1021/acsomega.7b00858
ACS Omega 2017, 2, 6063−6071

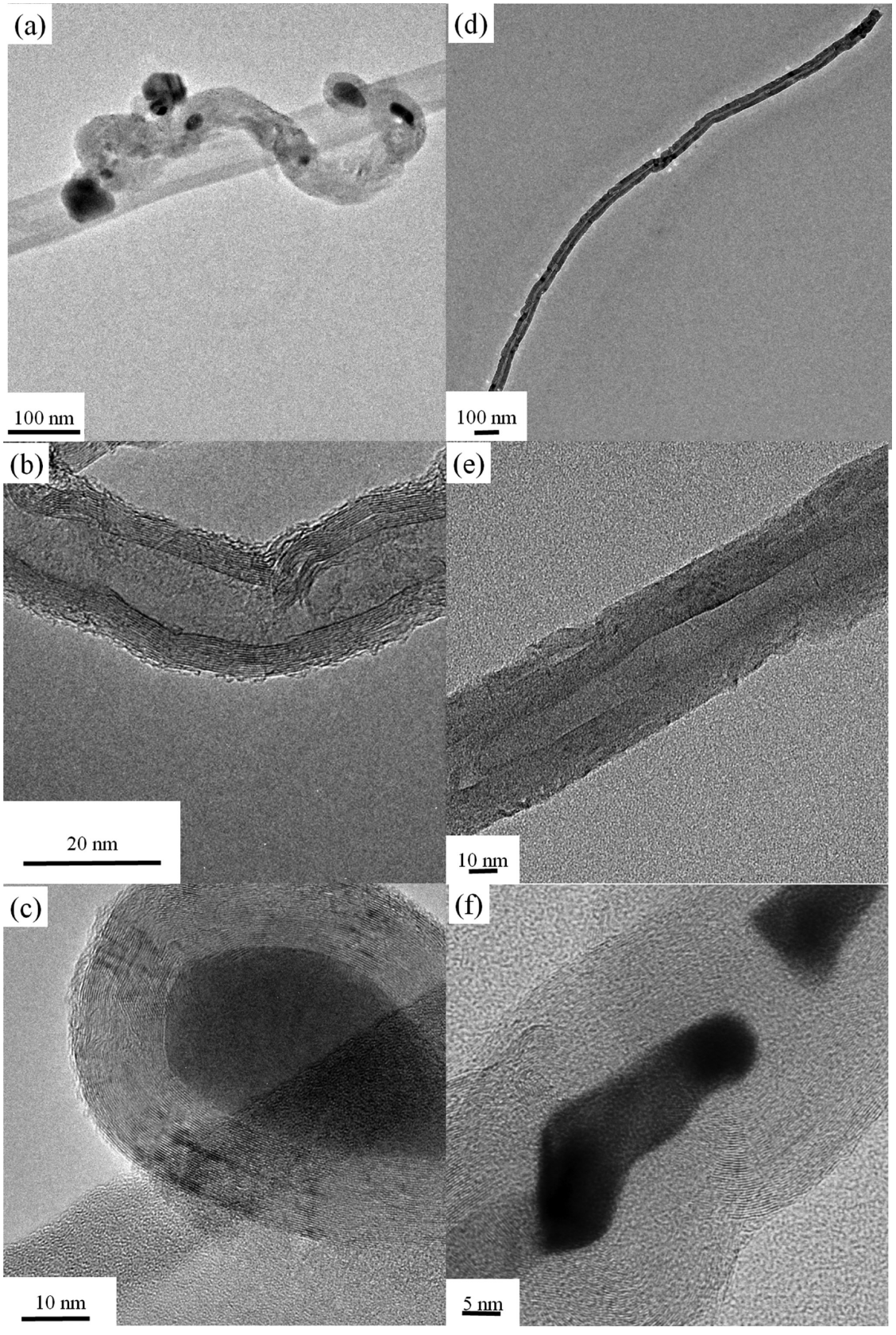

Figure 5. TEM images of CNTs grown at 860 °C on (a–c) bare Si and (d–f) 10 nm Ni substrates under different magnifications.

Ni and bare Si substrates, the metal clusters were wrapped by the multiwalled structure of CNTs, which suggests the close-ended structure of the CNTs. Because ferrocene is the sole catalyst source for CNTs grown on bare Si substrate, it can be speculated that the metal clusters observed in Figure 5a,c are iron catalyst clusters.[44] On the other hand, the metal clusters

DOI: 10.1021/acsomega.7b00858
ACS Omega 2017, 2, 6063–6071

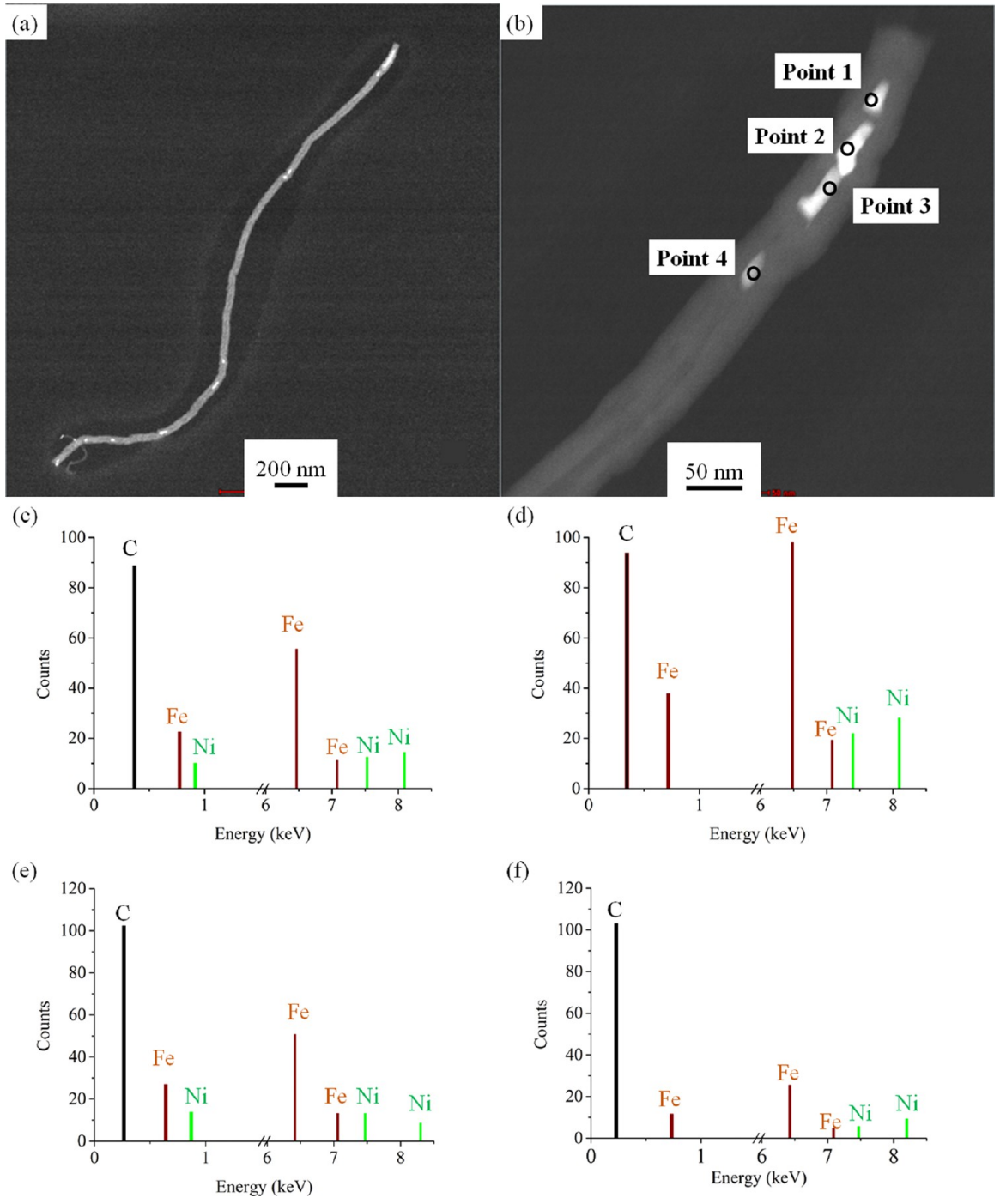

Figure 6. (a, b) STEM images of the CNTs grown on 10 nm Ni deposited substrate at different magnifications; TEM−EDS spectra at (c) point 1, (d) point 2, (e) point 3, and (f) point 4.

observed in Figure 5b,f may be comprised of both iron and nickel elements. This has been examined further in the following.

To determine the elements present in the metal clusters shown in Figure 5f, we performed EDS characterization at multiple points located on the cluster. The EDS characterization is carried out under scanning transmission electron microscopy (STEM) view to accurately locate the metal clusters embedded in the CNT body. As shown in Figure 6a, multiple metal clusters are found embedded in the CNT body, with an exceptionally large metal cluster found on the tip of the CNT. This embedded catalyst indicates a possible passivation of the catalyst by the CNT walls or amorphous carbon precipitation. EDS spectra are taken on four selected points of the CNT tip as shown in Figure 6b. From Figure 6c−f, both Fe and Ni elements are present from points 1−4. Exceptionally high signal counts from Ni at points 2 and 3 suggests the tip-growth mechanism of the CNTs from the Ni catalyst source, as agreed by Kim et al.[45] In summary, it is clear that both Ni and Fe catalysts involve in the CNT growth on 10 nm Ni-deposited substrates. From the EDS analysis shown in Figure 6, the nickel-rich metal cluster found on the CNT tip suggested the tip-growth mechanism of the CNTs by nickel catalyst. Besides, the larger diameter CNTs formed on 10 nm Ni substrate as

DOI: 10.1021/acsomega.7b00858
ACS Omega 2017, 2, 6063−6071

compared with those grown on bare Si substrate suggested the formation of larger catalyst particles on 10 nm Ni substrate during the CNT growth.[46]

The achievement of taller CNT heights by additional Ni catalyst can be attributed to the enhancement in the catalytic activity of the CNT growth. It has been well-reported that water-assisted CVD uses water molecules to oxidize the amorphous carbon formed on the catalyst particles, resulting in a prolonged catalyst lifetime.[27,47,48] On the other hand, Amama et al. reported that water reduces the Ostwald ripening behavior among the catalyst particles, enabling the formation of small, well-distributed catalyst particles, which favors the growth of tall CNTs.[49] In our current study, nickel/ferrocene-growth CNTs show a larger diameter than the CNTs grown from the sole ferrocene source. The formation of a larger CNT diameter indicates the formation of larger catalyst particles by the nickel ferrocene source, attributed to the additional nickel. Therefore, the anti-Ostwald ripening behavior mechanism of the water-assisted CVD may not be the most suitable approach in explaining the CNT growth enhancement in this study.

A possible mechanism to explain the achievement of taller CNTs by the additional Ni catalyst source is the increase in the CNT yield. It has been reported that adding Ni to Fe catalyst source results in a higher CNT yield.[29,50] This can be attributed to the increased rate of hydrocarbon decomposition by the additional Ni catalyst, as reported by Qian et al.[30] In our case, it can be speculated that adding Ni into the ferrocene catalyst source yields taller CNTs, possibly due to the improvement in the CNT yield by accelerating the hydrocarbon decomposition rate. In conjunction to the thicker CNTs formed by the additional Ni catalyst, it can be postulated that the formation of thicker CNTs is attributed to the formation of larger catalyst particles by Ni, whereas taller CNTs are due to the additional catalytic activity upon the addition of Ni catalyst. In summary, it has been demonstrated that adding nickel to the ferrocene catalyst source yields taller CNTs, possibly attributed to the higher hydrocarbon decomposition by the nickel/ferrocene catalyst source.

CONCLUSIONS

Tall, crystalline CNTs are grown using the nickel (Ni)/ferrocene-hybridized catalyst source. The results obtained conclusively show that the additional Ni catalyst source to ferrocene catalyst yields taller carbon nanotubes (CNTs). To obtain these results, the CNTs are grown on the Ni-deposited and bare Si substrates using a volatile catalyst (ferrocene/xylene) source chemical vapor deposition (CVD) at the growth temperatures ranging from 790 to 880 °C. It was found that the CNTs grown on bare Si substrate experience a reduction in the height at growth temperature above 860 °C. But the CNTs grown on 10 nm Ni substrates experience a continuous increase in the height as the growth temperature increases from 790 to 880 °C. The enhancement in the CNT heights by the additional Ni catalyst is also demonstrated on 5, 20, and 30 nm Ni layers. At the same time, the CNTs grown on both 10 nm Ni and bare Si substrates show a continuous improvement in the structural crystallinity with the increasing growth temperature, as reflected by the associated I_d/I_g ratios obtained from the Raman spectrum of the CNTs. These results together demonstrate the feasibility of a growing tall, crystalline CNTs using the nickel/ferrocene-hybridized catalyst source, which indicates a promising potential of this technique in the applications where these conditions are needed.

EXPERIMENTAL METHODS

N-doped silicon (Si) wafers are used as the substrates for all of the carbon nanotubes (CNTs) growth studies in this work. As a comparative study, the CNT growth is carried out on both 10 nm nickel (Ni) catalyst-deposited and bare Si substrates. In the preparation of 10 nm Ni-deposited substrates, 30 nm titanium followed by 50 nm titanium nitrate are first sputtered on the Si wafers as the barrier layer between the Ni catalyst and Si substrate. After that, 10 nm Ni catalyst is deposited on the titanium nitrate layer using the electron beam evaporation technique. The CNT growth processes are carried out on 10 nm Ni and bare Si substrates using an established volatile catalyst source (ferrocene/xylene) chemical vapor deposition (CVD) technique, described in the previous studies reported by our research group.[51−53] A typical CVD process is carried out in a 1/2 inch diameter quartz tube reactor in a continuous argon gas flow at temperatures of 790, 800, 820, 840, 860, and 880 °C under continuous injection of ferrocene/xylene solution. The ferrocene concentration in xylene solvent is fixed to be 1 wt %, the argon gas flow is fixed to be 100 sccm, and the growth duration is fixed at 60 s. At 880 °C growth temperature, it is found that the CNTs grown on 10 nm Ni substrate are significantly taller than those grown on bare Si substrate. After that, the CVD process using 880 °C growth temperature is then repeated on 5, 20, and 30 nm Ni-deposited substrates. The morphologies of the CNTs are characterized by field emission scanning electron microscopy (LEO 1550 Gemini SEM) and transmission electron microscopy (TEM, Philips Tecnai 20). The Raman spectra are measured using a single monochromator with a microscope micro-Raman spectroscopy system (WITec) with 532 nm laser wavelength.

AUTHOR INFORMATION

Corresponding Author

*E-mail: EBKTay@ntu.edu.sg. Tel: +65 6790 4533.

ORCID

Yu Dian Lim: 0000-0003-4188-997X

Beng Kang Tay: 0000-0002-3776-3648

Notes

The authors declare no competing financial interest.

ACKNOWLEDGMENTS

This work has been supported by the Office for Space Technology and Industry (OSTIn), Singapore, under the project S14-1126-NRF OSTIn-SRP; and COE Research Grant (M4081666).

REFERENCES

(1) Iijima, S. Helical Microtubules of Graphitic Carbon. *Nature* **1991**, *354*, 56−58.

(2) Yu, M.; et al. Strength and Breaking Mechanism of Multiwalled Carbon Nanotubes Under Tensile Load. *Science* **2000**, *287*, 637−640.

(3) Zhu, L.; Xu, J.; Xiu, Y.; Sun, Y.; Hess, D. W.; Wong, C. P. Growth and Electrical Characterization of High-Aspect-Ratio Carbon Nanotube Arrays. *Carbon* **2006**, *44*, 253−258.

(4) Ebbesen, T. W.; Lezec, H. J.; Hiura, H.; Bennett, J. W.; Ghaemi, H. F.; Thio, T. Electrical Conductivity of Individual Carbon Nanotubes. *Nature* **1996**, *382*, 54−56.

DOI: 10.1021/acsomega.7b00858
ACS Omega 2017, 2, 6063−6071

(5) Hazra, K. S.; Gigras, T.; Misra, D. S. Tailoring the Electrostatic Screening Effect during Field Emission from Hollow Multiwalled Carbon Nanotube Pillars. *Appl. Phys. Lett.* **2011**, *98*, No. 123116.
(6) Herrera-Herrera, A. V.; González-Curbelo, M. á.; Hernández-Borges, J.; Rodríguez-Delgado, M. á. Carbon Nanotubes Applications in Separation Science: A Review. *Anal. Chim. Acta* **2012**, *734*, 1−30.
(7) Li, H.; Xu, C.; Srivastava, N.; Banerjee, K. Carbon Nanomaterials for Next-Generation Interconnects and Passives: Physics, Status, and Prospects. *IEEE Trans. Electron Devices* **2009**, *56*, 1799−1821.
(8) Liu, L.; Ma, W.; Zhang, Z. Macroscopic Carbon Nanotube Assemblies: Preparation, Properties, and Potential Applications. *Small* **2011**, *7*, 1504−1520.
(9) Vardharajula, S.; Ali, S. Z.; Tiwari, P. M.; Eroğlu, E.; Vig, K.; Dennis, V. A.; Singh, S. R. Functionalized Carbon Nanotubes: Biomedical Applications. *Int. J. Nanomed.* **2012**, *7*, 5361−5374.
(10) Vollebregt, S.; Banerjee, S.; Tichelaar, F. D.; Ishihara, R. *Carbon Nanotubes TSV Grown on an Electrically Conductive ZrN Support Layer*. Proceedings of Interconnect Technology Conference, Grenoble, Italy, May 18−21, 2015.
(11) Vollebregt, S.; Banerjee, S.; Tichelaar, F. D.; Ishihara, R. The Growth of Carbon Nanotubes on Electrically Conductive ZrN Support Layers for through-Silicon Vias. *Microelectron. Eng.* **2016**, *156*, 126−130.
(12) de Heer, W. A.; Chatelain, A.; Ugarte, D. A Carbon Nanotube Field-Emission Electron Source. *Science* **1995**, *270*, 1179−1181.
(13) Patil, S. S.; Koinkar, P. M.; Dhole, S. D.; More, M. A.; Murakami, R. I. Influence of High-Energy Electron Irradiation on Field Emission Properties of Multi-Walled Carbon Nanotubes (MWCNTs) Films. *Phys. B* **2011**, *406*, 1809−1813.
(14) Pimenta, M. a.; Dresselhaus, G.; Dresselhaus, M. S.; Cançado, L. G.; Jorio, a.; Saito, R. Studying Disorder in Graphite-Based Systems by Raman Spectroscopy. *Phys. Chem. Chem. Phys.* **2007**, *9*, 1276−1291.
(15) Xie, R.; Zhang, C.; van der Veen, M. H.; Arstila, K.; Hantschel, T.; Chen, B.; Zhong, G.; Robertson, J. Carbon Nanotube Growth for through Silicon via Application. *Nanotechnology* **2013**, *24*, No. 125603.
(16) Rabbani, F. A.; Malaibari, Z. O.; Atieh, M. A.; Jamie, A. Catalytic Synthesis of Substrate-Free, Aligned and Tailored High Aspect Ratio Multiwall Carbon Nanotubes in an Ultrasonic Atomization Head CVD Reactor. *J. Nanomater.* **2016**, *2016*, 1−10.
(17) Kumar, M.; Ando, Y. Chemical Vapor Deposition of Carbon Nanotubes: A Review on Growth Mechanism and Mass Production. *J. Nanosci. Nanotechnol.* **2010**, *10*, 3739−3758.
(18) Zhou, Z.; Ci, L.; Song, L.; Yan, X.; Liu, D.; Yuan, H.; Gao, Y.; Wang, J.; Liu, L.; Zhou, W.; et al. The Intrinsic Temperature Effect of Raman Spectra of Double-Walled Carbon Nanotubes. *Chem. Phys. Lett.* **2004**, *396*, 372−376.
(19) Lee, C. J.; Park, J.; Huh, Y.; Yong Lee, J. Temperature Effect on the Growth of Carbon Nanotubes Using Thermal Chemical Vapor Deposition. *Chem. Phys. Lett.* **2001**, *343*, 33−38.
(20) Pint, C. Vertically Aligned Single-Walled Carbon Nanotube Growth from Iron-Molybdenum Catalyst; an Experiment and Modeling Approach to Why Deposition Order Matters. Master of Science Thesis, Rice University, Spring 2009.
(21) Bai, X.; Li, D.; Wang, Y.; Liang, J. Effects of Temperature and Catalyst Concentration on the Growth of Aligned Carbon Nanotubes. *Tsinghua Sci. Technol.* **2005**, *10*, 729−735.
(22) Allaedini, G.; Tasirin, S. M.; Aminayi, P.; Yaakob, Z.; MeowTalib, M. Z. Carbon Nanotubes via Different Catalysts and the Important Factors That Affect Their Production: A Review on Catalyst Preferences. *Int. J. Nano Dimens.* **2016**, *7*, 186−200.
(23) Magrez, A.; Seo, J. W.; Smajda, R.; Mionić, M.; Forró, L. Catalytic CVD Synthesis of Carbon Nanotubes: Towards High Yield and Low Temperature Growth. *Materials* **2010**, *3*, 4871−4891.
(24) Xiang, R.; Yang, Z.; Zhang, Q.; Luo, G.; Qian, W.; Wei, F.; Kadowaki, M.; Einarsson, E.; Maruyama, S. Growth Deceleration of Vertically Aligned Carbon Nanotube Arrays: Catalyst Deactivation or Feedstock Diffusion Controlled? *J. Phys. Chem. C* **2008**, *112*, 4892−4896.
(25) Schünemann, C.; Schäffel, F.; Bachmatiuk, A.; Queitsch, U.; Sparing, M.; Rellinghaus, B.; Lafdi, K.; Schultz, L.; Büchner, B.; Rümmeli, M. H. Catalyst Poisoning by Amorphous Carbon during Carbon Nanotube Growth: Fact or Fiction? *ACS Nano* **2011**, *5*, 8928−8934.
(26) Hata, K.; Futaba, D. N.; Mizuno, K.; Namai, T.; Yumura, M.; Iijima, S. Water-Assisted Highly Efficient Synthesis of Impurity-Free Single-Walled Carbon Nanotubes. *Science* **2004**, *306*, 1362−1364.
(27) Patole, S. P.; Alegaonkar, P. S.; Lee, H.-C.; Yoo, J.-B. Optimization of Water Assisted Chemical Vapor Deposition Parameters for Super Growth of Carbon Nanotubes. *Carbon* **2008**, *46*, 1987−1993.
(28) Liu, J.; Shen, A.; Wei, X.; Zhou, K.; Chen, W.; Chen, F.; Xu, J.; Wang, S.; Dai, L. Ultrathin Wrinkled N-Doped Carbon Nanotubes for Noble-Metal Loading and Oxygen Reduction Reaction. *ACS Appl. Mater. Interfaces* **2015**, *7*, 20507−20512.
(29) Fazle Kibria, A. K. M.; Mo, Y. H.; Nahm, K. S.; Kim, M. J. Synthesis of Narrow-Diameter Carbon Nanotubes from Acetylene Decomposition over an Iron-Nickel Catalyst Supported on Alumina. *Carbon* **2002**, *40*, 1241−1247.
(30) Qian, W.; Liu, T.; Wang, Z.; Yu, H.; Li, Z.; Wei, F.; Luo, G. Effect of Adding Nickel to Iron-Alumina Catalysts on the Morphology of as-Grown Carbon Nanotubes. *Carbon* **2003**, *41*, 2487−2493.
(31) Atthipalli, G.; Epur, R.; Kumta, P. N.; Gray, J. L. Nickel Catalyst-Assisted Vertical Growth of Dense Carbon Nanotube Forests on Bulk Copper. *J. Phys. Chem. C* **2011**, *115*, 3534.
(32) Atthipalli, G.; Epur, R.; Kumta, P. N.; Gray, J. L. Ferrocene and Inconel Assisted Growth of Dense Carbon Nanotube Forests on Copper Foils. *J. Vac. Sci. Technol., B: Microelectron. Nanometer Struct.−Process., Meas., Phenom.* **2011**, *29*, No. 04D102.
(33) Meyyappan, M.; Delzeit, L.; Cassell, A.; Hash, D. Carbon Nanotube Growth by PECVD: A Review. *Plasma Sources Sci. Technol.* **2003**, *12*, 205−216.
(34) Ramirez, A.; Latorre, N.; Mallada, R.; Tiggelaar, R. M.; Monzón, A. Unraveling the Growth of Vertically Aligned Multi-Walled Carbon Nanotubes by Chemical Vapor Deposition. *Mater. Res. Express* **2014**, *1*, No. 045604.
(35) Niemann, D. L.; Silan, J.; Killian, J. L.; Schwanfelder, K. R.; Rahman, M.; Meyyappan, M.; Nguyen, C. V. *Carbon Nanotube Field Emission Devices with Integrated Gate for High Current Applications*. Proceedings of the 2008 8th IEEE Conference on Nanotechnology, Arlington, TX, USA, Aug 18−21, 2008.
(36) Bokobza, L.; Zhang, J. Raman Spectroscopic Characterization of Multiwall Carbon Nanotubes and of Composites. *eXPRESS Polym. Lett.* **2012**, *6*, 601−608.
(37) Hoyos-Palacio, L. M.; García, aG; Pérez-Robles, J. F.; González, J.; Martínez-Tejada, H. V. Catalytic Effect of Fe, Ni, Co and Mo Onthe CNTs Production. *IOP Conf. Ser.: Mater. Sci. Eng.* **2014**, *59*, No. 012005.
(38) Geng, X.; Cen, Y.; Sisson, R. D.; Liang, J. An Effective Approach towards the Immobilization of PtSn Nanoparticles on Noncovalent Modified Multi-Walled Carbon Nanotubes for Ethanol Electro-oxidation. *Energies* **2016**, *9*, 165.
(39) Moulton, K.; Morrill, N. B.; Konneker, A. M.; Jensen, B. D.; Vanfleet, R. R.; Allred, D. D.; Davis, R. C. Effect of Iron Catalyst Thickness on Vertically Aligned Carbon Nanotube Forest Straightness for CNT-MEMS. *J. Micromech. Microeng.* **2012**, *22*, No. 055004.
(40) Srivastava, S. K.; Vankar, V. D.; Kumar, V. *Effect of Catalyst Film Thickness on the Growth, Microstructure and Field Emission Characteristics of Carbon Nanotubes*. IEEE International Workshop on Physics of Semiconductor Devices, Mumbai, India, 2007; pp 1−4.
(41) Mohammad Haniff, M. A. S.; Lee, H. W.; Lee, W. Y.; Bien, D. C. S.; Wahid, K. A.; Lee, M. W.; Azid, I. A. Investigation of Low-Pressure Bimetallic Cobalt-Iron Catalyst-Grown Multiwalled Carbon Nanotubes and Their Electrical Properties. *J. Nanomater.* **2013**, *2013*, No. 637939.
(42) Jang, Y.-T.; Ahn, J.-H.; Lee, Y.-H.; Ju, B.-K. Effect of NH3 and Thickness of Catalyst on Growth of Carbon Nanotubes Using

DOI: 10.1021/acsomega.7b00858
ACS Omega 2017, 2, 6063−6071

Thermal Chemical Vapor Deposition. *Chem. Phys. Lett.* **2003**, *372*, 745−749.
(43) Kar, R.; Sarkar, S. G.; Basak, C. B.; Patsha, A.; Dhara, S.; Ghosh, C.; Ramachandran, D.; Chand, N.; Chopade, S. S.; Patil, D. S. Effect of Substrate Heating and Microwave Attenuation on the Catalyst Free Growth and Field Emission of Carbon Nanotubes. *Carbon* **2015**, *94*, 256−265.
(44) Yah, C. S.; Iyuke, S. E.; Simate, G. S.; Unuabonah, E. I.; Bathgate, G.; Matthews, G.; Cluett, J. D. Continuous Synthesis of Multiwalled Carbon Nanotubes from Xylene Using the Swirled Floating Catalyst Chemical Vapor Deposition Technique. *J. Mater. Res.* **2011**, *26*, 640−644.
(45) Kim, K. J.; Yu, W.-R.; Youk, J. H.; Lee, J. Factors Governing the Growth Mode of Carbon Nanotubes on Carbon-Based Substrates. *Phys. Chem. Chem. Phys.* **2012**, *14*, 14041−14048.
(46) Abdi, Y.; Koohsorkhi, J.; Derakhshandeh, J.; Mohajerzadeh, S.; Hoseinzadegan, H.; Robertson, M. D.; Bennett, J. C.; Wu, X.; Radamson, H. PECVD-Grown Carbon Nanotubes on Silicon Substrates with a Nickel-Seeded Tip-Growth Structure. *Mater. Sci. Eng., C* **2006**, *26*, 1219−1223.
(47) Hata, K.; Futaba, D. N.; Mizuno, K.; Namai, T.; Yumura, M.; Iijima, S. Water-Assisted Highly Efficient Synthesis of Impurity-Free Single-Walled Carbon Nanotubes. *Science* **2004**, *306*, 1362−1364.
(48) Yamada, T.; Maigne, A.; Yudasaka, M.; Mizuno, K.; Futaba, D. N.; Yumura, M.; Iijima, S.; Hata, K. Revealing the Secret of Water-Assisted Carbon Nanotube Synthesis by Microscopic Observation of the Interaction of Water on the Catalysts. *Nano Lett.* **2008**, *8*, 4288−4292.
(49) Amama, P. B.; Pint, C. L.; McJilton, L.; Kim, S. M.; Stach, E. a.; Murray, P. T.; Hauge, R. H.; Maruyama, B. Role of Water in Super Growth of Single-Walled Carbon Nanotube Carpets. *Nano Lett.* **2009**, *9*, 44−49.
(50) Kibria, A. K. M. F.; Mo, Y. H.; Nahm, K. S. Synthesis of Carbon Nanotubes over Nickel−Iron Catalysts Supported on Alumina under Controlled Conditions. *Catal. Lett.* **2001**, *71*, 229−236.
(51) Dian, Y.; Hu, L.; Vasiliyvich, A.; Grapov, D.; Tay, K.; Aditya, S.; Miao, J.; Labunov, V. Temperature-Dependent Selective Growth of Carbon Nanotubes in Si/SiO_2 Structures for Field Emitter Array Applications. *Mater. Res. Bull.* **2017**, *95*, 129−137.
(52) Lim, Y. D.; Alexander, A.; Grapov, D.; Tay, B. K.; Aditya, S.; Labunov, V. *Field Emission Characteristics of Short CNT Bundles*. IEEE International Vacuum Electronics Conference, 2016.
(53) Serbun, P.; Muller, G.; Tymoshchyk, A.; Kashko, I.; Shulitski, B.; Labunov, V. *High Field Emission Current Density from Structured CNT Bundle Cathodes*. International Vacuum Nanoelectronics Conference, 2013; pp 1−2.

DOI: 10.1021/acsomega.7b00858
ACS Omega 2017, 2, 6063−6071